



Cite this: RSC Adv., 2017, 7, 52227

Synthesis and structure–activity relationship of N^4 -benzylamine- N^2 -isopropyl-quinazoline-2,4-diamines derivatives as potential antibacterial agents

Zhengyun Jiang,^a W. David Hong,^{bcde} Xiping Cui,^a Hongcan Gao,^a Panpan Wu,^{ad} Yingshan Chen,^a Ding Shen,^a Yang Yang,^a Bingjie Zhang,^a Mark J. Taylor,^b Stephen A. Ward,^b Paul M. O'Neill,^c Suging Zhao^{id *a} and Kun Zhang^{*ade}

A series of N^4 -benzylamine- N^2 -isopropyl-quinazoline-2,4-diamine derivatives has been synthesized and tested for antibacterial activity against five bacterial strains. Twelve different substituents on the N^4 -benzylamine group have been investigated along with replacement of the quinazoline core (with either a benzothiophene or regiosomeric pyridopyrimidine ring systems). In order to develop structure activity relationships, all derivatives were tested for their antibacterial activities against *Escherichia coli* and *Staphylococcus aureus* via Kirby–Bauer assays and minimum inhibitory concentration assays. Eight of the most potent compounds against *S. aureus* and *E. coli* were also screened against one strain of methicillin-resistant *S. aureus* (MRSA), *Staphylococcus epidermidis* and *Salmonella typhimurium* to further examine their antibacterial activities. Lead compound A5 showed good activities with MICs of $3.9 \mu\text{g mL}^{-1}$ against *E. coli*, *S. aureus* and *S. epidermidis* and $7.8 \mu\text{g mL}^{-1}$ against MRSA. Selected front runners were also screened for their DMPK properties *in vitro* to assess their potential for further development.

Received 18th September 2017
Accepted 26th October 2017

DOI: 10.1039/c7ra10352h

rsc.li/rsc-advances

Introduction

Novel antibacterial chemotypes are urgently needed because of the emergence and spread of multidrug resistant microorganisms and pathogenic bacterial infections.^{1,2} *Staphylococcus aureus* is the most common pathogen of surgical site and wound infections.³⁻⁶ Antibiotic-resistant strains of *S. aureus* infections often occur in epidemic waves that are initiated by one, or a few, successful clones.⁷⁻⁹ Every year in the United States approximately two million people fall ill and 23 000 people die because of antibiotic-resistant bacterial infections, according to a report from the Center for Diseases Control and Prevention.^{10,11} Antibiotic-resistant bacterial strains, in particular methicillin-resistant *S. aureus* (MRSA) infection rates remain constant within the community and hospital settings in U.S.¹²⁻¹⁴ Worryingly, strains of *S. aureus* showing extended resistance to vancomycin, daptomycin, linezolid and

ceftaroline, which are used to treat MRSA infections, have been reported recently in the literature.¹⁵⁻¹⁸ MRSA is on the list of bacteria for which new antibiotics are urgently needed as recognized by World Health Organization in 2017.¹⁹

Quinazolines and derivatives have shown attractive antibacterial activity.²⁰⁻²² In previous studies, quinazoline-based compounds have been investigated for their potential antibacterial activity, especially anti-MRSA activity. Bedi *et al.* (2004) reported 2,4-disubstituted quinazoline, such as compound A (Fig. 1), displayed antibacterial activity against a wide spectrum of bacteria including *S. aureus*, and *E. coli*.²³ Chandrika *et al.* (2010) reported the *in vitro* activity of multiple fluoro-substituted triazol-4-yl substituted quinazoline B (Fig. 1) against *S. aureus* and *S. epidermidis* with an MIC of 9.375 μ g mL⁻¹.²⁴ Van Horn *et al.* (2014) have reported *N*²,*N*⁴-disubstituted quinazoline-2,4-diamines such as C (Fig. 1) that

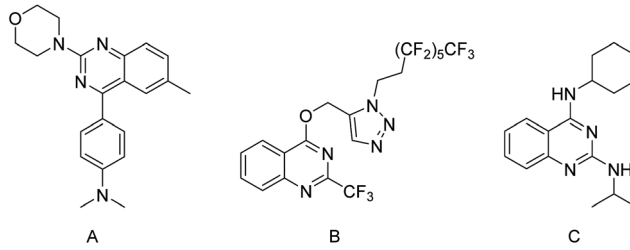


Fig. 1 Quinazolines with reported antibacterial activity.

displayed *in vitro* and *in vivo* activities against *S. aureus*, a low potential for spontaneous resistance and low toxicity.²⁵ Furthermore, this proof-of-concept work opened up opportunities for further investigation of quinazoline-2,4-diamines in terms of structural activity relationships against a broader spectrum of bacteria strains and DMPK related parameters. In this work, we designed a library of 2,4-diaminoquinazoline analogues and closely related derivatives, including thirteen 2,4-diaminoquinazolines, thirteen 2,4-diaminothieno[3,2-*d*]pyrimidines, six 2,4-diaminopyrido[3,2-*d*]pyrimidine derivatives and six 2,4-diaminopyrido[2,3-*d*]pyrimidine derivatives. These compounds are structurally distinct from previously reported quinazoline core antibacterials. These compounds have been used to further explore how the structural variation affects antibacterial activity. Herein, a structure–activity relationship (SAR) study is reported which focuses on the substituent of *N*⁴-benzylamine and the variations of the quinazoline scaffold.

All derivatives were tested against *S. aureus* and *E. coli* in Kirby–Bauer assays initially. The antibacterial potency of active compounds was further determined by minimum inhibitory concentrations (MICs) assays. Further MICs assays were performed against methicillin-resistant *S. aureus* (MRSA), *Staphylococcus epidermidis* and *Salmonella typhimurium* to evaluate the spectrum of antibacterial activity of the most active compounds. In addition, DMPK related properties, such as lipophilicity ($\log D_{7.4}$), aqueous solubility and *in vitro* metabolic stability were also assessed for a selected group of compounds to illustrate how the structural modifications can potentially influence the pharmacokinetics of these new lead molecules.

Results and discussion

Chemistry

To systematically explore structure–activity relationships, a group of *N*⁴-benzylamine-*N*²-isopropyl-quinazoline-2,4-diamine derivatives which include four chemical subsets of

compounds with different heterocyclic aromatic rings fused to the pyrimidine ring in the scaffold were designed and then subsequently synthesized *via* adapted methods from the literature (Fig. 2).^{25–30} Commercially available compound (a) was reacted with phosphorus oxychloride and phosphorus pentachloride resulting in the corresponding 2,4-dichloro intermediates (b). Substitution with benzylamines occurred selectively at the 4-position, yielding 4-benzylamino-2-chloroquinazoline (c) under mild conditions. Next, substitution at the 2-position with isopropyl amine gave the desired 2,4-diamino products (d). The synthesis of compounds from series A and B were started from the commercially available as quinazoline-2,4(1*H*,3*H*)-dione and thieno[3,2-*d*]pyrimidine-2,4(1*H*,3*H*)-dione, respectively. However, 2,4-dichloropyrido[3,2-*d*]pyrimidine and 2,4-dichloropyrido[2,3-*d*]pyrimidine, exemplified as intermediate (b) which were readily acquired commercially have been used in the synthesis of series C and D compounds. Throughout the synthetic routes, all intermediates have been purified and the final *N*⁴-benzylamine-*N*²-isopropyl-quinazoline-2,4-diamines derivatives have been characterized by ¹H NMR, ¹³C NMR and high resolution mass spectrum.

Structure–activity relationship study

Initially all 4 chemical subsets (series A–D) were tested for their activities in inhibiting bacterial growth in the Kirby–Bauer assay against *E. coli* and *S. aureus*. Active compounds with zones of inhibitions (ZOIs) ≥ 7.0 mm in the Kirby–Bauer assay were then tested for their minimum inhibitory concentrations (MICs) to quantify their potency against *E. coli* and *S. aureus* (Table 1). The data of ZOIs and MICs presented are the average results from three independent experiments.

Kirby–Bauer assay

Kirby–Bauer assay was used to test the compounds at a single concentration of 5 mg mL^{−1} to determine whether they

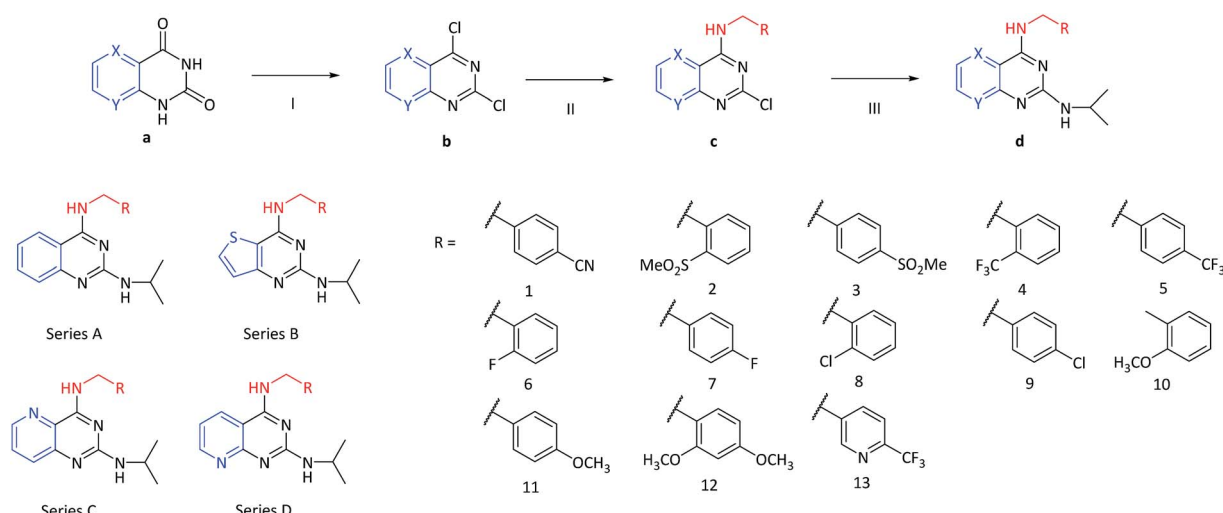


Fig. 2 Synthetic route and chemical structures of *N*⁴-benzylamino-*N*²-isopropyl-quinazoline-2,4-diamines. Reagents and conditions: (I) PCl_5 , POCl_3 , 120 °C, 6 h; (II) substituted benzylamine, triethylamine, THF, rt, overnight; (III) isopropylamine, 1,4-dioxane, 120 °C, 48 h.

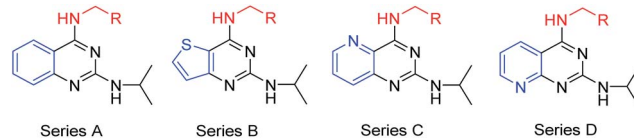
Table 1 Antibacterial activities of *N*²-isopropyl-*N*⁴-benzylamine-quinazoline-2,4-diamines derivatives

Compound code	R	<i>E. coli</i> ^a		<i>S. aureus</i> ^b	
		ZoIs (mm)	MICs (μg mL ⁻¹)	ZoIs (mm)	MICs (μg mL ⁻¹)
A1	4-CN-phenyl-	20.2 ± 0.6	31.2	11.8 ± 0.5	31.2
A2	2-SO ₂ Me-phenyl-	8.3 ± 0.2	125.0	8.1 ± 0.2	62.5
A3	4-SO ₂ Me-phenyl-	7.5 ± 0.3	≥125.0	None	NT
A4	2-CF ₃ -phenyl-	20.4 ± 0.7	15.6	16.2 ± 0.7	3.9
A5	4-CF ₃ -phenyl-	22.4 ± 0.1	3.9	13.2 ± 0.5	3.9
A6	2-F-phenyl-	23.8 ± 0.8	15.6	12.4 ± 0.3	15.6
A7	4-F-phenyl-	22.3 ± 0.5	15.6	14.5 ± 0.3	7.8
A8	2-Cl-phenyl-	21.2 ± 0.7	15.6	12.0 ± 0.5	3.9
A9	4-Cl-phenyl-	18.6 ± 0.2	7.8	11.6 ± 0.2	3.9
A10	2-OCH ₃ -phenyl-	15.7 ± 0.6	31.2	17.4 ± 0.5	31.2
A11	4-OCH ₃ -phenyl-	17.1 ± 0.9	31.2	15.4 ± 0.4	7.8
A12	3,4-Di-OCH ₃ -phenyl-	16.2 ± 0.4	31.2	14.6 ± 0.5	15.6
A13	4-CN-phenyl-	21.0 ± 0.4	31.2	11.6 ± 0.3	31.2
B1	2-SO ₂ Me-phenyl-	7.2 ± 0.1	≥125.0	8.9 ± 0.3	62.5
B2	4-SO ₂ Me-phenyl-	7.9 ± 0.2	≥125.0	None	NT
B3	2-CF ₃ -phenyl-	None ^c	NT ^d	None	NT
B4	4-CF ₃ -phenyl-	16.8 ± 0.8	31.2	12.1 ± 0.3	7.8
B5	2-F-phenyl-	8.6 ± 0.1	125.0	12.7 ± 0.3	7.8
B6	4-F-phenyl-	8.0 ± 0.3	62.5	11.1 ± 0.5	31.2
B7	2-Cl-phenyl-	8.5 ± 0.4	62.5	10.9 ± 0.3	31.2
B8	4-Cl-phenyl-	11.4 ± 0.4	62.5	13.6 ± 0.6	15.6
B9	2-OCH ₃ -phenyl-	8.1 ± 0.5	62.5	12.9 ± 0.4	7.8
B10	4-OCH ₃ -phenyl-	None	NT	None	NT
B11	3,4-Di-OCH ₃ -phenyl-	None	NT	None	NT
B12	4-CN-phenyl-	None	NT	9.2 ± 0.4	62.5
B13	2-SO ₂ Me-phenyl-	7.3 ± 0.1	≥125.0	8.2 ± 0.1	62.5
C1	4-SO ₂ Me-phenyl-	None	NT	7.6 ± 0.3	62.5
C2	4-CF ₃ -phenyl-	None	NT	None	NT
C3	4-CN-phenyl-	None	NT	None	NT
C5	2-SO ₂ Me-phenyl-	None	NT	8.5 ± 0.6	15.6
C13	4-SO ₂ Me-phenyl-	None	NT	None	NT
D1	4-CF ₃ -phenyl-	None	NT	None	NT
D2	4-CF ₃ -pyridyl-	None	NT	8.1 ± 0.2	31.2
D3	4-CF ₃ -pyridyl-	None	NT	None	NT
D5	4-CF ₃ -pyridyl-	None	NT	10.2 ± 0.1	7.8
D13	4-CF ₃ -pyridyl-	None	NT	8.1 ± 0.8	62.5
Norfloxacin		NT	≤0.12	NT	0.24
Vancomycin		NT	>31.2	NT	0.98
Methicillin		NT	>31.2	NT	0.49

^a *Escherichia coli*, CMCC 44102. ^b *Staphylococcus aureus*, ATCC 6538. ^c No zone of inhibition was determined. ^d Not tested.

inhibited bacterial growth. The data are exhibited in Table 1. In this assay, sterile filter disks with a diameter of 6 mm were used. The diameter of ZOIs greater than 10.0 mm was defined as strongly active, 7.0–10.0 mm was weakly active, and less than 7.0 mm was inactive. As shown in Fig. 3, 13 compounds all from series A or B appear in the green area which signifies compounds showing potent activity against both Gram-negative bacteria, *E. coli* and Gram-positive bacteria *S. aureus*. In the left-hand side yellow area, 5 compounds from series B and D showed some activity against Gram-positive *S. aureus* but weak

activity against Gram-negative *E. coli*. No compound showed noticeably stronger activity against Gram-negative *E. coli* than Gram-positive *S. aureus*, represented by the blue coloured area in Fig. 3. From this analysis, it also indicated that while a number of series A quinazoline analogues have activities against both Gram-positive and Gram-negative bacteria, series B thieno[3,2-*d*]pyrimidines were more biased to Gram-positive bacteria and series C and D compounds had limited activities in inhibiting the growth of these bacterial strains.



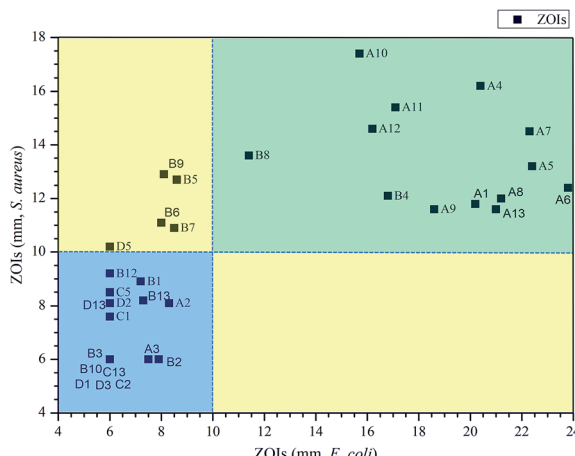


Fig. 3 Zones of inhibition (ZOIs) in Kirby–Bauer assays against *E. coli* and *S. aureus*.

Minimum inhibitory concentrations (MICs) assay

All N^4 -benzylamine- N^2 -isopropyl-quinazoline-2,4-diamines derivatives with measurable ZOIs in the Kirby–Bauer assays were tested in minimum inhibitory concentration (MIC) assays against the same two strains of bacteria to quantitatively determine their antibacterial potency. Norfloxacin, vancomycin and methicillin were used as positive controls.

In general, the results of the MIC assay mirrored the results from the single concentration Kirby–Bauer assay, and the antibacterial potency of the chemical series are in the order of quinazolines > thieno[3,2-*d*]pyrimidines > pyrido[3,2-*d*]pyrimidines \approx pyrido[2,3-*d*]pyrimidines, while higher potency was observed against Gram-positive *S. aureus* than against Gram-negative *E. coli*. (Table 1). In the most active subset, series A, substitutions on the benzene ring in the N^4 -benzylamin side-chain had a significant effect of the potency of compounds. Lipophilic electron withdrawing group substitution in this side-chain, such as CF_3 and Cl were beneficial for antibacterial activity. On the other hand, the more polar substitutions *i.e.* SO_2Me or CN were not tolerated (A1–3). Similar observations were also seen after the incorporation of an additional nitrogen in this side-chain (A13) which reduced both lipophilicity ($\log D$) and potency compared with the corresponding analogue A5 without the nitrogen (further discussion regarding the effect of the structural modifications to the physiochemical properties are described in a following session). Series A analogues, with substitutions at the *para*-position of the benzene ring, were more potent against Gram-negative *E. coli* than the corresponding *ortho*-substituted analogues, but these substitutions had little effect on potency against Gram-positive *S. aureus* (A4 vs. A5 and A8 vs. A9). Quinazoline derivative A5 with a trifluoromethyl group at the *para*-position of the benzene ring was the most active compound in this subset of compounds and indeed in this whole set of compounds with $\text{MICs} = 3.9 \mu\text{g mL}^{-1}$ against both Gram-positive and negative bacteria, *S. aureus* and *E. coli*. It was closely followed by the chloro-substituted analogue at the same position (A9) that has the

same potency against *S. aureus* but slightly reduced potency ($\text{MIC} = 7.8 \mu\text{g mL}^{-1}$) against Gram-negative *E. coli*. The series B thieno[3,2-*d*]pyrimidine analogues also showed some activity against both strains of bacteria, but they were less active than their corresponding quinazoline core analogues in general. The SAR observed in series B compounds is very similar to the SAR of series A. While the replacement of the quinazoline core to a theino[3,2-*d*]pyrimidine core had less effect on the potency against Gram-positive *S. aureus* (2–4 fold reductions), this modification resulted in a noticeable reduction of antibacterial activity against Gram-negative *E. coli* (2–32 fold reductions). Compounds in both series C and D with an additional nitrogen incorporated into the 5- or 8-position of the quinazoline core showed significantly reduced potency against both strains of bacteria. Two compounds with $p\text{-CF}_3$ substitutions on the N^4 -benzylamine side-chain (C5 and D5) in these two series showed moderate activities against *S. aureus* ($\text{MIC} = 15.6 \mu\text{g mL}^{-1}$ and $7.8 \mu\text{g mL}^{-1}$, respectively), but no activity against *E. coli*.

The MIC assay was used to evaluate the eight most active compounds against *S. aureus* (as described above) namely, A4, A5, A7–9, A11, B5 and, B9 against a strain of MRSA. MICs of these selected compounds against MRSA were only two to four folds higher than the corresponding MICs against the susceptible strain of *S. aureus*. The MIC difference seen with this group of compounds is similar to the MIC differences seen with the two positive controls, *i.e.* Norfloxacin and vancomycin (2–3 folds), but is significantly less than that seen with methicillin (~ 16 folds). These results suggest that this new class of compound has minimal cross resistance with this strain of MRSA although further studies are required to formally confirm this using a broader range of MRSA lines with unique and well characterized resistance mechanisms. The most potent compound against this strain of MRSA was A5, the $p\text{-CF}_3$ substituted analogue from series A.

In order to extend our understanding of the antibacterial activities of this class of compounds, the same group of eight active compounds from series A and B were also tested against additional strains of Gram-positive and Gram-negative bacteria, namely *S. epidermidis* and *S. typhimurium* using the MIC assay. Overall the antibacterial activities of these eight selected compounds against these additional bacterial lines matched very well with those against *S. aureus* and *E. coli* (Table 2). Most of the tested compounds showed good activities against Gram-positive *S. epidermidis* at similar levels to those observed with *S. aureus*, but their potency against Gram-negative *S. typhimurium* was considerably lower than their potency against other tested strains of bacteria. Both quinazoline analogues with CF_3 substituted at either *ortho*- or *para*-positions in the N^4 -benzylamine side-chain (A4 and A5) were the most potent compounds from the assays against *S. epidermidis* and *S. typhimurium* with $\text{MIC} = 3.9 \mu\text{g mL}^{-1}$ and $15.6 \mu\text{g mL}^{-1}$, respectively.

Physicochemical properties and *in vitro* metabolic stability studies

Along with the SAR studies of these compounds, selected derivatives were also evaluated for their DMPK properties



Table 2 Antibacterial activities of the most active compounds against MRSA, *S. epidermidis* and *S. typhimurium*

Compound	MRSA ^a	<i>S. epidermidis</i> ^b	<i>S. typhimurium</i> ^c
	MICs ($\mu\text{g mL}^{-1}$)	MICs ($\mu\text{g mL}^{-1}$)	MICs ($\mu\text{g mL}^{-1}$)
A4	15.6	3.9	15.6
A5	7.8	3.9	15.6
A7	31.2	7.8	15.6
A8	15.6	7.8	62.5
A9	15.6	7.8	15.6
A11	31.2	15.6	31.2
B5	15.6	7.8	≥ 125.0
B9	15.6	7.8	31.2
Norfloxacin	0.97	1.95	≤ 0.12
Vancomycin	1.95	3.9	≥ 31.2
Methicillin	7.8	0.24	≥ 31.2

^a Methicillin-resistant *Staphylococcus aureus* (MRSA), ATCC 43300.^b *Staphylococcus epidermidis*, ATCC 12228. ^c *Salmonella typhimurium*, CMCC 50115.

including physicochemical properties such as $\log D_{7.4}$, aqueous solubility and plasma protein binding, and *in vitro* metabolic stability against human microsome and rat hepatocytes (Table 3). Overall, the more active compounds, such as A4, A5, A8 and A9 showed high lipophilicity ($\log D_{7.4}$) and low aqueous solubility in PBS buffer. Replacing the benzene ring of quinazoline scaffold with a thiophene ring (B5 vs. A5 and B9 vs. A9) did not alter lipophilicity but increased the aqueous solubility slightly. Incorporation of nitrogens in different parts of the molecules (A5 vs. A13 or D5) or replacement of CF_3 group with an OMe group (A5 vs. A11) resulted in reductions of lipophilicity and improvement of solubility, but all manipulations resulted in decreased antibacterial activities. Based on the available SAR and the data of $\log D_{7.4}$ in Table 3, it suggested there is a potential positive correlation between lipophilicity and antibacterial activity. Compounds A4, A5, A8, A9, B5 and B9, which have $\log D_{7.4}$ values higher than 4, showed good activities against *S. aureus* with MICs = $3.9 \mu\text{g mL}^{-1}$. On the contrary, compounds A7, A11 and A13, which have $\log D_{7.4}$ values from 3.3 to 3.6, showed a 2-fold or 8-fold less active against the same

bacterium. The percentage of human plasma protein binding for those measured compounds also showed positive correlation with lipophilicity. Although the plasma protein bindings are in the relatively high range of percentage (96.5–99.9%) it is not uncommon for anti-infective agents. In terms of metabolic stability, most of the quinazoline analogues showed acceptable stability *in vitro* against both human microsome and rat hepatocytes, and are more stable than the corresponding thieno-pyrimidine analogues (A5 vs. B5 and A9 vs. B9). The azaquinazoline analogue D5 had the best *in vitro* metabolic stability against both human microsome and rat hepatocytes, but this modification was not well tolerated in the antibacterial SAR.

Conclusions

In this article, 36 N^2,N^4 -disubstituted quinazoline-2,4-diamines and closely related derivatives with potential antibacterial activity were designed and synthesized. Our SAR study demonstrated that lipophilic electron withdrawing groups, such as trifluoromethyl and chloro, in the N^4 -benzylamine side-chain were beneficial for antibacterial potency, while substitution at the 4-position of the benzene ring was advantageous compared with substitutions at the 2-position. Changing the quinazoline scaffold to a thieno[3,2-*d*]pyrimidine, series B compounds, still showed limited antibacterial activity compared with the corresponding quinazoline analogues. Scaffold morphing to pyrido[3,2-*d*]pyrimidine or pyrido[2,3-*d*]pyrimidine was not tolerated in the SAR and most of the compounds bearing these two cores were significantly less potent than the parent quinazolines. Screens against one strain of MRSA suggested this class of compounds had limited cross resistance to methicillin although the exact protein target(s) for this class of compounds needs to be further investigated against a broader selection of MRSA bacteria. The results from the screens against *S. aureus* and *E. coli* in the SAR study and the additional screens against *S. epidermidis* and *S. typhimurium* demonstrated a broad spectrum of antibacterial activity against both Gram-positive and Gram-negative bacteria while the potency against Gram-positive bacteria was generally higher than the latter. The *in vitro* DMPK screening results suggested

Table 3 Physicochemical properties and *in vitro* metabolic stability

Compound	$\log D_{7.4}$	Aq. Sol. ^a (μM)	H. Mics CL _{int} ^b ($\mu\text{l min}^{-1}$ mg)	R. Heps CL _{int} ^c ($\mu\text{l min}^{-1}$ per 10^6 cells)	H. PPB ^d %
A4	4.6	0.2	9.2	25	99.6
A5	4.7	0.5	29	45	99.8
A7	3.6	27	32	37	98.0
A8	4.2	5	19	98	98.9
A9	4.3	4	36	51	99.2
A11	3.3	40	37	>300	97.4
A13	3.3	17	45	7.8	96.5
B5	4.5	3.7	70	76	99.9
B9	4.8	11	156	217	99.8
D5	4.4	3	7.6	6.5	98.5

^a Aqueous solubility in pH 7.4 PBS. ^b Human microsomes intrinsic clearance. ^c Rat hepatocytes intrinsic clearance. ^d Human plasma protein binding.

that some of the lead series A quinazolines had acceptable metabolic stability *in vitro*, their physiochemical properties, aqueous solubility in particular would need to be improved if they were to be developed further. The most active compound A5 showed good potency against *E. coli*, *S. aureus*, *S. epidermidis*, *S. typhimurium* and MRSA. Although the cytotoxicity of these series of compounds were not determined yet, the cytotoxicity of some closed analogues were reported by our group and others (Van Horn 2014, Devine 2015 and Johnston 2017), and there is no obvious risk of cytotoxicity for these chemotypes in general.^{25,31,32} Further investigation of cytotoxicity of selected leads will be carried out in the next stage of optimisation and evaluation to mitigate any potential risk in this area. The results from this work indicate the potential of this chemical series and directions for further investigation of this chemotype as potential antibacterial agents.

Experimental

All chemicals, reagents and solvents were obtained from commercial sources and used without further purification. ¹H and ¹³C NMR spectra were recorded on a Bruker Avance III 400 MHz Superconducting Fourier system in the solvent indicated. Chemical shifts were reported in units of ppm on the delta (δ) scale and coupling constants (J) were reported in units of Hz. Data for ¹H NMR were reported as follows: chemical shift (δ ppm), multiplicity (s = singlet, d = doublet, t = triplet, q = quartet, m = multiplet), integration and coupling constant (Hz), while ¹³C NMR analyses were reported in terms of chemical shift. Thin-layer chromatography was performed on silica gel 60 F254 aluminium sheets from Merck KGaA. Melting points were determined by using a microscopic melting point instrument and were uncorrected. High resolution mass spectra (HRMS) were performed on a Bruker maXis impact system.

General method for the synthesis of compounds A, B, C, D

General synthetic procedures I. One equivalent of quinazoline-2,4-dione and three equivalents of phosphorus pentachloride were mixed in 10 equivalents of phosphorus oxychloride and the mixture refluxed for 6 hours under a nitrogen atmosphere. After that the mixture was cooled down to room temperature and added with ice in the amount of 10–15 times the reaction volume. The solution was extracted with ethyl acetate three times and the combined organic phase was dried over anhydrous magnesium sulfate. The organic phase was filtered and concentrated to give crude product under reduced pressure. The crude product was purified by flash chromatography with petroleum ether and ethyl acetate.

General synthesis procedure II. Benzylamine (1.2 equivalent) and triethylamine (2 equivalent) were mixed with 1 equivalent of 2,4-dichloroquinazoline in tetrahydrofuran and stirred overnight at room temperature, after that it was concentrated under reduced pressure. The remaining residue was purified by flash chromatography with petroleum ether and ethyl acetate.

General synthesis procedure III. Isopropylamine (4 equivalent) and 4-benzylamino-substituted 2-chloroquinazoline (1

equivalent) were mixed in 5 mL 1,4-dioxane in a high pressure reactor and heated to 120 °C for 48 h. The high pressure reactor was cooled down and the solution was concentrated under reduced pressure. The remaining residue was purified by flash chromatography with dichloromethane and methanol.

A1 *N*⁴-(4-Cyanobenzyl)-*N*²-isopropylquinazoline-2,4-diamine. Yellow solid; yield, 75%; R_f = 0.36 (9 : 1 dichloromethane to methanol); ¹H NMR (400 MHz, DMSO-d₆) δ 10.35 (s, 1H), 8.38 (s, 1H), 7.80 (d, J = 8.3 Hz, 2H), 7.78–7.72 (m, 1H), 7.59 (d, J = 8.2 Hz, 2H), 7.37 (s, 1H), 4.84 (d, J = 5.5 Hz, 2H), 4.06 (s, 1H), 1.08 (s, 6H). ¹³C NMR (100 MHz, DMSO-d₆) δ 159.90, 158.94, 144.21, 139.90, 138.89, 135.05, 132.28, 128.26, 128.17, 124.24, 123.70, 118.75, 109.73, 62.76, 42.89, 22.03. HRMS: m/z calcd for C₁₉H₂₀N₅ [M + H]⁺ 318.1713; found 318.1719. Melting point 257–260 °C.

A2 *N*²-Isopropyl-*N*⁴-(2-(methylsulfonyl)benzyl)quinazoline-2,4-diamine. Brown solid; yield, 49%; R_f = 0.42 (9 : 1 dichloromethane to methanol); ¹H NMR (400 MHz, CDCl₃) δ 8.04 (dd, J = 7.9, 1.3 Hz, 1H), 7.71 (dd, J = 7.6, 0.8 Hz, 1H), 7.64–7.56 (m, 2H), 7.55–7.47 (m, 2H), 7.39 (d, J = 8.0 Hz, 1H), 7.14–7.08 (m, 1H), 5.15 (d, J = 5.6 Hz, 2H), 4.29 (m, 1H), 3.18 (s, 3H), 1.27 (d, J = 6.5 Hz, 6H). ¹³C NMR (100 MHz, CDCl₃) δ 160.11, 156.10, 146.37, 137.59, 137.55, 133.57, 133.36, 129.09, 129.02, 127.57, 122.05, 122.00, 120.69, 109.96, 43.48, 42.45, 41.53, 21.67. HRMS: m/z calcd for C₁₉H₂₃N₄O₂S [M + H]⁺ 371.1536; found 371.1540. Melting point 171–173 °C.

A3 *N*²-Isopropyl-*N*⁴-(4-(methylsulfonyl)benzyl)quinazoline-2,4-diamine. Brown solid; yield, 53%; R_f = 0.39 (9 : 1 dichloromethane to methanol); ¹H NMR (400 MHz, CDCl₃) δ 8.01 (d, J = 6.9 Hz, 1H), 7.73 (d, J = 8.3 Hz, 2H), 7.50–7.47 (m, 2H), 7.46 (d, J = 7.2 Hz, 1H), 7.32 (d, J = 8.3 Hz, 1H), 7.07 (t, J = 7.6 Hz, 1H), 4.85 (s, 2H), 4.07 (m, 1H), 2.97 (s, 3H), 1.109 (d, J = 6.4 Hz, 6H). ¹³C NMR (100 MHz, CDCl₃) δ 160.52, 155.15, 151.64, 145.21, 139.02, 134.17, 128.10, 127.42, 122.94, 122.67, 119.93, 110.00, 44.37, 44.11, 43.14, 22.25. HRMS: m/z calcd for C₁₉H₂₃N₄O₂S [M + H]⁺ 371.1536; found 371.1539. Melting point 175–177 °C.

A4 *N*²-Isopropyl-*N*⁴-(2-(trifluoromethyl)benzyl)quinazoline-2,4-diamine. Yellow solid; yield, 26%; R_f = 0.29 (9 : 1 dichloromethane to methanol); ¹H NMR (400 MHz, DMSO-d₆) δ 10.01 (s, 1H), 8.35 (s, 1H), 7.76 (d, J = 7.8 Hz, 1H), 7.74 (d, J = 10.0 Hz, 1H), 7.61 (t, J = 7.5 Hz, 1H), 7.50 (d, J = 8.1 Hz, 1H), 7.47 (d, J = 7.6 Hz, 1H), 7.33 (s, 1H), 4.95 (d, J = 4.4 Hz, 2H), 4.01–3.83 (m, 1H), 1.02 (dd, J = 22.3, 15.7 Hz, 6H). ¹³C NMR (100 MHz, DMSO-d₆) δ 163.46, 162.50, 160.05, 150.15, 138.99, 136.68, 136.03, 132.66, 131.96, 127.73, 127.34, 126.61, 126.15, 125.85, 125.80, 123.17, 42.54, 41.04, 21.93. HRMS: m/z calcd for C₁₉H₂₀F₃N₄ [M + H]⁺ 361.1635; found 361.1639. Melting point 231–233 °C.

A5 *N*²-Isopropyl-*N*⁴-(4-(trifluoromethyl)benzyl)quinazoline-2,4-diamine. Yellow solid; yield, 19%; R_f = 0.47 (9 : 1 dichloromethane to methanol); ¹H NMR (400 MHz, CDCl₃) δ 7.65 (d, J = 8.0 Hz, 1H), 7.52 (t, J = 5.6 Hz, 2H), 7.48 (dd, J = 6.9, 1.2 Hz, 1H), 7.42 (d, J = 4.5 Hz, 2H), 7.41 (s, 1H), 7.07–7.00 (m, 1H), 6.62 (s, 1H), 4.82 (d, J = 5.0 Hz, 3H), 4.17 (m, 1H), 1.14 (d, J = 6.5 Hz, 6H). ¹³C NMR (100 MHz, CDCl₃) δ 160.21, 158.84, 151.97, 143.19, 133.03, 129.75, 127.92, 125.65, 125.29, 122.92, 121.17, 121.01, 110.72, 44.59, 42.88, 23.26. HRMS: m/z calcd for



$C_{19}H_{20}F_3N_4$ [M + H]⁺ 361.1635; found 361.1639. Melting point 69–71 °C.

A6 *N⁴-(2-Fluorobenzyl)-N²-isopropylquinazoline-2,4-diamine.* Yellow oil; yield, 89%; R_f = 0.32 (9 : 1 dichloromethane to methanol); ¹H NMR (400 MHz, CDCl₃) δ 8.04 (d, J = 5.6 Hz, 1H), 7.51 (t, J = 7.7 Hz, 1H), 7.36 (t, J = 7.1 Hz, 2H), 7.19 (d, J = 7.8 Hz, 1H), 7.17 (dd, J = 4.7, 2.8 Hz, 1H), 7.05–7.00 (m, 1H), 6.98 (d, J = 10.0 Hz, 1H), 4.86 (d, J = 3.5 Hz, 2H), 4.14 (ddd, J = 18.0, 12.2, 5.3 Hz, 3H), 1.15 (d, J = 6.7 Hz, 6H). ¹³C NMR (100 MHz, CDCl₃) δ 163.65, 162.04, 160.65, 160.43, 159.59, 152.91, 134.92, 129.74, 129.39, 124.56, 124.32, 124.11, 115.55, 109.62, 43.83, 40.46, 22.46. HRMS: m/z calcd for C₁₈H₂₀N₄ [M + H]⁺ 311.1667; found 311.1669.

A7 *N⁴-(4-Fluorobenzyl)-N²-isopropylquinazoline-2,4-diamine.* Yellow solid; yield, 83%; R_f = 0.29 (9 : 1 dichloromethane to methanol); ¹H NMR (400 MHz, CDCl₃) δ 9.71 (s, NH), 8.49 (s, NH), 7.47 (t, J = 7.7 Hz, 1H), 7.37 (dd, J = 8.3, 5.5 Hz, 2H), 7.25 (d, J = 5.7 Hz, 1H), 7.14 (t, J = 7.6 Hz, 1H), 6.87 (t, J = 8.6 Hz, 2H), 4.80 (s, 2H), 4.17 (m, 1H), 1.18 (d, J = 6.5 Hz, 5H). ¹³C NMR (100 MHz, CDCl₃) δ 163.51, 161.07, 160.22, 134.50, 133.60, 129.77, 129.69, 123.62, 115.66, 115.45, 109.87, 63.88, 44.75, 43.69, 22.72. HRMS: m/z calcd for C₁₈H₂₀N₄ [M + H]⁺ 311.1667; found 311.1669. Melting point 240–243 °C.

A8 *N⁴-(2-Chlorobenzyl)-N²-isopropylquinazoline-2,4-diamine.* Yellow solid; yield, 39%; R_f = 0.31 (9 : 1 dichloromethane to methanol); ¹H NMR (400 MHz, CDCl₃) δ 8.19–8.13 (m, 1H), 7.58 (td, J = 7.2, 3.2 Hz, 1H), 7.42 (d, J = 7.0 Hz, 1H), 7.37–7.27 (m, 3H), 7.21–7.15 (m, 2H), 4.90 (d, J = 2.3 Hz, 2H), 4.13 (m, 1H), 1.14 (d, J = 6.5 Hz, 6H). ¹³C NMR (100 MHz, CDCl₃) δ 160.37, 152.21, 138.98, 135.00, 134.60, 133.02, 129.48, 128.69, 128.56, 126.88, 124.39, 123.67, 116.89, 109.49, 43.79, 43.03, 21.97. HRMS: m/z calcd for C₁₈H₂₀ClN₄ [M + H]⁺ 327.1371; found 327.1374. Melting point 209–212 °C.

A9 *N⁴-(4-Chlorobenzyl)-N²-isopropylquinazoline-2,4-diamine.* Yellow oil; yield, 94%; R_f = 0.26 (9 : 1 dichloromethane to methanol); ¹H NMR (400 MHz, CDCl₃) δ 8.09 (d, J = 7.7 Hz, 1H), 7.49 (t, J = 7.7 Hz, 1H), 7.35 (d, J = 8.3 Hz, 1H), 7.29 (d, J = 8.4 Hz, 2H), 7.22 (d, J = 8.4 Hz, 2H), 7.14 (t, J = 7.5 Hz, 1H), 6.21–6.09 (m, 2H), 4.76 (s, 2H), 4.14 (dt, J = 11.4, 5.0 Hz, 1H), 1.19 (d, J = 6.5 Hz, 6H). ¹³C NMR (100 MHz, CDCl₃) δ 172.91, 160.45, 152.77, 139.19, 136.22, 134.97, 133.35, 129.25, 128.74, 124.31, 116.95, 109.75, 44.85, 43.89, 22.51. HRMS: m/z calcd for C₁₈H₂₀ClN₄ [M + H]⁺ 327.1371; found 327.1373.

A10 *N²-Isopropyl-N⁴-(2-methoxybenzyl)quinazoline-2,4-diamine.* White solid; yield, 70%; R_f = 0.31 (9 : 1 dichloromethane to methanol); ¹H NMR (400 MHz, CDCl₃) δ 7.87 (d, J = 7.4 Hz, 1H), 7.51 (t, J = 7.7 Hz, 1H), 7.38 (d, J = 8.2 Hz, 1H), 7.28 (d, J = 7.2 Hz, 1H), 7.23 (d, J = 7.8 Hz, 1H), 7.18 (t, J = 7.6 Hz, 1H), 6.87 (d, J = 6.6 Hz, 1H), 6.85 (d, J = 6.6 Hz, 1H), 4.84 (d, J = 5.0 Hz, 2H), 4.23 (m, 6.3 Hz, 1H), 3.88 (s, 3H), 1.25 (d, J = 6.5 Hz, 6H). ¹³C NMR (100 MHz, CDCl₃) δ 160.09, 157.57, 134.60, 129.89, 129.42, 129.18, 125.18, 123.71, 122.98, 120.91, 120.76, 110.75, 110.58, 109.71, 55.59, 43.78, 41.41, 22.62. HRMS: m/z calcd for C₁₉H₂₃N₄O [M + H]⁺ 323.1866; found 323.1870. Melting point 138–140 °C.

A11 *N²-Isopropyl-N⁴-(4-methoxybenzyl)quinazoline-2,4-diamine.* Yellow solid; yield, 73%; R_f = 0.31 (9 : 1

dichloromethane to methanol); ¹H NMR (400 MHz, CDCl₃) δ 8.29 (s, 1H), 7.45 (t, J = 7.7 Hz, 1H), 7.35 (d, J = 8.6 Hz, 2H), 7.27 (d, J = 10.2 Hz, 1H), 7.13 (t, J = 7.6 Hz, 1H), 6.77 (d, J = 8.4 Hz, 2H), 4.78 (d, J = 4.2 Hz, 2H), 4.24 (m, 1H), 3.73 (s, 3H), 1.24 (d, J = 6.5 Hz, 6H). ¹³C NMR (100 MHz, CDCl₃) δ 160.18, 160.11, 159.21, 134.63, 129.80, 129.56, 129.51, 123.97, 114.26, 114.21, 114.08, 110.01, 55.41, 44.98, 43.81, 22.72. HRMS: m/z calcd for C₁₉H₂₃N₄O [M + H]⁺ 323.1866; found 323.1869. Melting point 208–210 °C.

A12 *N⁴-(3,4-Dimethoxybenzyl)-N²-isopropylquinazoline-2,4-diamine.* Yellow solid; yield, 15%; R_f = 0.39 (9 : 1 dichloromethane to methanol); ¹H NMR (400 MHz, CDCl₃) δ 8.24 (s, 1H), 7.44 (t, J = 7.7 Hz, 1H), 7.27 (d, J = 10.7 Hz, 1H), 7.11 (t, J = 7.6 Hz, 1H), 7.04 (d, J = 1.3 Hz, 1H), 6.95 (dd, J = 8.2, 1.4 Hz, 1H), 6.74 (d, J = 8.2 Hz, 1H), 4.77 (s, 2H), 4.25 (m, 1H), 3.81 (s, 3H), 3.80 (s, 3H), 1.24 (d, J = 6.4 Hz, 6H). ¹³C NMR (100 MHz, CDCl₃) δ 160.19, 154.16, 149.26, 148.68, 148.65, 134.36, 130.48, 130.02, 123.87, 123.56, 120.57, 111.85, 111.31, 110.13, 56.08, 56.05, 45.27, 43.66, 22.75. HRMS: m/z calcd for C₂₀H₂₅N₄O₂ [M + H]⁺ 353.1972; found 353.1976. Melting point 192–194 °C.

A13 *N²-Isopropyl-N⁴-((6-(trifluoromethyl)pyridin-3-yl)methyl)quinazoline-2,4-diamine.* Yellow solid; yield, 23%; R_f = 0.39 (9 : 1 dichloromethane to methanol); ¹H NMR (400 MHz, CD₃OD) δ 8.78 (s, 1H), 8.08 (d, J = 6.3 Hz, 1H), 8.07 (s, 1H), 7.79 (d, J = 8.1 Hz, 1H), 7.70 (t, J = 7.7 Hz, 1H), 7.43 (d, J = 8.1 Hz, 1H), 7.33 (t, J = 7.7 Hz, 1H), 4.95 (s, 2H), 4.12 (dq, J = 12.5, 6.3 Hz, 1H), 1.17 (d, J = 6.4 Hz, 6H). ¹³C NMR (101 MHz, CD₃OD) δ 162.08, 155.98, 150.39, 147.70, 144.62, 139.76, 138.25, 135.77, 124.75, 124.37, 121.72, 121.70, 120.28, 111.44, 44.59, 43.34, 22.71. HRMS: m/z calcd for C₁₉H₂₀F₃N₄ [M + H]⁺ 362.1587; found 362.1590. Melting point 202–205 °C.

B1 *N⁴-(4-Cyanobenzyl)-N²-isopropylthieno[3,2-d]pyrimidine-2,4-diamine.* Yellow oil; yield, 61%; R_f = 0.31 (9 : 1 dichloromethane to methanol); ¹H NMR (400 MHz, CDCl₃) δ 7.63–7.58 (m, 2H), 7.56 (d, J = 5.3 Hz, 1H), 7.46 (d, J = 8.4 Hz, 2H), 7.11 (d, J = 5.3 Hz, 1H), 5.43 (s, NH), 4.96 (s, NH), 4.84 (d, J = 5.8 Hz, 2H), 4.07 (m, 1H), 1.16 (d, J = 6.5 Hz, 6H). ¹³C NMR (100 MHz, CDCl₃) δ 161.09, 160.16, 157.48, 144.78, 132.52, 131.18, 128.13, 123.67, 118.88, 111.28, 106.04, 44.43, 43.23, 23.13. HRMS: m/z calcd for C₁₇H₁₇N₅S [M + H]⁺ 324.1277; found 324.1281.

B2 *N²-Isopropyl-N⁴-(2-(methylsulfonyl)benzyl)thieno[3,2-d]pyrimidine-2,4-diamine.* Yellow oil; yield, 38%; R_f = 0.53 (9 : 1 dichloromethane to methanol); ¹H NMR (400 MHz, CDCl₃) δ 8.03–7.99 (m, 1H), 7.72 (d, J = 7.5 Hz, 1H), 7.56 (t, J = 7.4 Hz, 1H), 7.50 (d, J = 5.3 Hz, 1H), 7.44 (t, J = 7.6 Hz, 1H), 7.04 (d, J = 5.3 Hz, 1H), 5.88 (s, 1H), 5.10 (d, J = 6.3 Hz, 2H), 4.70 (d, J = 8.0 Hz, 1H), 4.17 (dq, J = 13.0, 6.5 Hz, 1H), 3.14 (s, 3H), 1.20 (d, J = 6.5 Hz, 6H). ¹³C NMR (100 MHz, CDCl₃) δ 161.70, 160.53, 157.18, 138.64, 138.40, 134.08, 131.84, 130.89, 129.79, 128.40, 123.72, 106.24, 45.10, 42.99, 42.05, 23.21. HRMS: m/z calcd for C₁₇H₂₀N₂NaO₂S₂ [M + Na]⁺ 399.0920; found 399.0925.

B3 *N²-Isopropyl-N⁴-(4-(methylsulfonyl)benzyl)thieno[3,2-d]pyrimidine-2,4-diamine.* Yellow oil; yield, 31%; R_f = 0.56 (9 : 1 dichloromethane to methanol); ¹H NMR (400 MHz, CDCl₃) δ 7.80 (d, J = 8.3 Hz, 2H), 7.52 (d, J = 5.3 Hz, 1H), 7.49 (d, J = 8.2 Hz, 2H), 7.07 (d, J = 5.3 Hz, 1H), 5.82 (s, 1H), 4.82 (d, J = 5.9 Hz, 2H), 4.75 (d, J = 7.9 Hz, 1H), 4.05 (dq, J = 13.1, 6.5 Hz,



1H), 3.00 (s, 3H), 1.12 (d, J = 6.5 Hz, 6H). ^{13}C NMR (100 MHz, CDCl_3) δ 161.70, 160.46, 157.44, 146.04, 139.18, 130.98, 128.27, 127.59, 123.78, 106.06, 44.61, 44.08, 43.05, 23.12. HRMS: m/z calcd for $\text{C}_{17}\text{H}_{20}\text{N}_2\text{NaO}_2\text{S}_2$ [M + Na]⁺ 399.0920; found 399.0924.

B4 *N²-Isopropyl-N⁴-(2-(trifluoromethyl)benzyl)thieno[3,2-d]pyrimidine-2,4-diamine.* Yellow solid; yield, 39%; R_f = 0.33 (9 : 1 dichloromethane to methanol); ^1H NMR (400 MHz, CD_3OD) δ 7.77 (d, J = 5.4 Hz, 1H), 7.68 (d, J = 7.7 Hz, 1H), 7.52 (d, J = 4.3 Hz, 2H), 7.38 (dt, J = 8.1, 4.1 Hz, 1H), 7.03 (d, J = 5.4 Hz, 1H), 4.95 (s, 2H), 4.00–3.89 (m, 1H), 1.04 (d, J = 6.5 Hz, 6H). ^{13}C NMR (100 MHz, CD_3OD) δ 161.85, 161.69, 159.04, 139.67, 133.28, 133.27, 132.88, 128.90, 127.95, 126.81, 123.49, 107.34, 43.87, 41.71, 23.02. HRMS: m/z calcd for $\text{C}_{17}\text{H}_{18}\text{F}_3\text{N}_4\text{S}$ [M + H]⁺ 367.1199; found 367.1203. Melting point 135–137 °C.

B5 *N²-Isopropyl-N⁴-(4-(trifluoromethyl)benzyl)thieno[3,2-d]pyrimidine-2,4-diamine.* Brown solid; yield, 47%; R_f = 0.31 (9 : 1 dichloromethane to methanol); ^1H NMR (400 MHz, CDCl_3) δ 7.53 (d, J = 8.2 Hz, 2H), 7.50 (d, J = 5.3 Hz, 1H), 7.43 (d, J = 8.1 Hz, 2H), 7.07 (d, J = 5.3 Hz, 1H), 5.97 (s, 1H), 5.14 (s, 1H), 4.81 (d, J = 5.6 Hz, 2H), 4.09 (dq, J = 13.2, 6.5 Hz, 1H), 1.15 (d, J = 6.5 Hz, 6H). ^{13}C NMR (100 MHz, CDCl_3) δ 161.49, 160.45, 157.54, 143.25, 130.91, 129.96, 127.89, 125.69, 123.81, 122.91, 105.96, 44.39, 43.17, 23.16. HRMS: m/z calcd for $\text{C}_{17}\text{H}_{18}\text{F}_3\text{N}_4\text{NaS}$ [M + Na]⁺ 389.1018; found 389.1016. Melting point 62–64 °C.

B6 *N⁴-(2-Fluorobenzyl)-N²-isopropylthieno[3,2-d]pyrimidine-2,4-diamine.* Yellow oil; yield, 49%; R_f = 0.51 (9 : 1 dichloromethane to methanol); ^1H NMR (400 MHz, CDCl_3) δ 7.50 (d, J = 5.3 Hz, 1H), 7.38 (t, J = 7.6 Hz, 1H), 7.23 (m, 1H), 7.10–7.01 (m, 3H), 5.54 (s, NH), 5.16 (s, NH), 4.83 (d, J = 5.3 Hz, 2H), 4.16 (td, J = 13.0, 6.5 Hz, 1H), 1.20 (d, J = 6.5 Hz, 6H). ^{13}C NMR (100 MHz, CDCl_3) δ 162.35, 159.96, 157.55, 130.98, 130.01, 129.21, 125.82, 124.28, 123.25, 115.56, 115.35, 106.21, 43.19, 38.67, 23.14. HRMS: m/z calcd for $\text{C}_{16}\text{H}_{18}\text{FN}_4\text{S}$ [M + H]⁺ 317.1231; found 317.1234.

B7 *N⁴-(4-Fluorobenzyl)-N²-isopropylthieno[3,2-d]pyrimidine-2,4-diamine.* Yellow oil; yield, 58%; R_f = 0.56 (9 : 1 dichloromethane to methanol); ^1H NMR (400 MHz, CDCl_3) δ 7.48 (dd, J = 5.3, 0.6 Hz, 1H), 7.29 (dd, J = 8.2, 5.5 Hz, 2H), 7.04 (d, J = 5.3 Hz, 1H), 6.96 (t, J = 8.3 Hz, 2H), 5.94 (s, 1H), 5.06 (s, 1H), 4.71 (d, J = 4.6 Hz, 2H), 4.13 (td, J = 13.4, 6.5 Hz, 1H), 1.17 (d, J = 6.4 Hz, 6H). ^{13}C NMR (100 MHz, CDCl_3) δ 163.24, 160.80, 159.34, 157.42, 134.63, 131.31, 129.40, 129.32, 122.55, 115.30, 106.33, 43.95, 43.12, 22.97. HRMS: m/z calcd for $\text{C}_{16}\text{H}_{18}\text{FN}_4\text{S}$ [M + H]⁺ 317.1231; found 317.1234.

B8 *N⁴-(2-Chlorobenzyl)-N²-isopropylthieno[3,2-d]pyrimidine-2,4-diamine.* Yellow oil; yield, 28%; R_f = 0.33 (9 : 1 dichloromethane to methanol); ^1H NMR (400 MHz, CDCl_3) δ 7.48 (d, J = 5.3 Hz, 1H), 7.39 (dd, J = 5.0, 4.2 Hz, 1H), 7.34 (dd, J = 5.8, 3.5 Hz, 1H), 7.19–7.17 (m, 1H), 7.16 (d, J = 5.1 Hz, 1H), 7.06 (d, J = 5.3 Hz, 1H), 4.84 (d, J = 5.9 Hz, 2H), 4.13 (dq, J = 19.5, 6.5 Hz, 1H), 1.16 (d, J = 6.5 Hz, 6H). ^{13}C NMR (100 MHz, CDCl_3) δ 160.61, 160.09, 157.43, 136.19, 133.37, 130.89, 129.56, 129.45, 128.60, 126.89, 123.30, 106.14, 43.05, 42.46, 23.06. HRMS: m/z calcd for $\text{C}_{16}\text{H}_{18}\text{ClN}_4\text{S}$ [M + H]⁺ 333.0935; found 333.0935.

B9 *N⁴-(4-Chlorobenzyl)-N²-isopropylthieno[3,2-d]pyrimidine-2,4-diamine.* Yellow oil; yield, 50%; R_f = 0.38 (9 : 1 dichloromethane to methanol); ^1H NMR (400 MHz, CDCl_3) δ 7.52 (d, J =

5.3 Hz, 1H), 7.32–7.24 (m, 4H), 7.09 (d, J = 5.3 Hz, 1H), 5.65 (b, 1H), 5.32 (b, 1H), 4.74 (d, J = 5.6 Hz, 2H), 4.14 (dq, J = 13.1, 6.5 Hz, 1H), 1.20 (d, J = 6.5 Hz, 6H). ^{13}C NMR (100 MHz, CDCl_3) δ 161.77, 160.61, 157.46, 137.62, 133.07, 130.67, 129.07, 128.72, 123.86, 106.00, 44.02, 43.03, 23.18. HRMS: m/z calcd for $\text{C}_{16}\text{H}_{18}\text{ClN}_4\text{S}$ [M + H]⁺ 333.0935; found 333.0938.

B10 *N²-Isopropyl-N⁴-(2-methoxybenzyl)thieno[3,2-d]pyrimidine-2,4-diamine.* Yellow solid; yield, 37%; R_f = 0.31 (9 : 1 dichloromethane to methanol); ^1H NMR (400 MHz, CDCl_3) δ 7.47 (d, J = 5.3 Hz, 1H), 7.34 (dd, J = 7.4, 1.3 Hz, 1H), 7.28–7.22 (m, 1H), 7.07 (d, J = 5.3 Hz, 1H), 6.91 (d, J = 7.4 Hz, 1H), 6.88 (d, J = 7.9 Hz, 1H), 5.42 (s, 1H), 4.82 (d, J = 7.8 Hz, 1H), 4.78 (d, J = 5.8 Hz, 2H), 4.22 (qd, J = 13.0, 6.5 Hz, 1H), 3.86 (s, 3H), 1.23 (d, J = 6.5 Hz, 6H). ^{13}C NMR (100 MHz, CDCl_3) δ 161.31, 160.61, 157.71, 157.67, 130.25, 129.75, 128.80, 126.80, 123.81, 120.64, 110.49, 106.25, 55.41, 43.02, 40.55, 23.23. HRMS: m/z calcd for $\text{C}_{17}\text{H}_{21}\text{N}_4\text{OS}$ [M + H]⁺ 329.1431; found 329.1434. Melting point 60–62 °C.

B11 *N²-Isopropyl-N⁴-(4-methoxybenzyl)thieno[3,2-d]pyrimidine-2,4-diamine.* Yellow oil; yield, 51%; R_f = 0.22 (9 : 1 dichloromethane to methanol); ^1H NMR (400 MHz, CDCl_3) δ 7.49 (d, J = 5.3 Hz, 1H), 7.29 (d, J = 8.5 Hz, 2H), 7.09 (d, J = 5.3 Hz, 1H), 6.86 (d, J = 8.6 Hz, 2H), 5.17 (s, 1H), 4.77 (d, J = 7.8 Hz, 1H), 4.70 (d, J = 5.5 Hz, 2H), 4.20 (m, 1H), 3.79 (s, 3H), 1.22 (d, J = 6.5 Hz, 6H). ^{13}C NMR (100 MHz, CDCl_3) δ 160.71, 159.18, 157.54, 131.00, 130.45, 129.29, 123.97, 114.20, 106.10, 55.41, 44.42, 43.08, 23.27. HRMS: m/z calcd for $\text{C}_{17}\text{H}_{21}\text{N}_4\text{OS}$ [M + H]⁺ 329.1431; found 329.1432.

B12 *N⁴-(3,4-Dimethoxybenzyl)-N²-isopropylthieno[3,2-d]pyrimidine-2,4-diamine.* Yellow solid; yield, 51%; R_f = 0.24 (9 : 1 dichloromethane to methanol); ^1H NMR (400 MHz, CDCl_3) δ 7.52 (d, J = 5.3 Hz, 1H), 7.10 (d, J = 5.3 Hz, 1H), 6.92 (m, 2H), 6.86–6.81 (m, 1H), 5.05 (s, 1H), 4.83 (s, 1H), 4.71 (d, J = 5.4 Hz, 2H), 4.21 (td, J = 13.1, 6.5 Hz, 1H), 3.87 (s, 3H), 3.85 (s, 3H), 1.24 (d, J = 6.5 Hz, 6H). ^{13}C NMR (100 MHz, CDCl_3) δ 161.33, 160.52, 157.58, 149.40, 148.77, 131.41, 130.66, 123.88, 120.37, 111.54, 111.52, 106.15, 56.14, 56.07, 44.95, 43.18, 23.28. HRMS: m/z calcd for $\text{C}_{18}\text{H}_{23}\text{N}_4\text{O}_2\text{S}$ [M + H]⁺ 359.1536; found 359.1542. Melting point 134–136 °C.

B13 *N²-Isopropyl-N⁴-(6-(trifluoromethyl)pyridin-3-yl)methyl)thieno[3,2-d]pyrimidine-2,4-diamine.* Yellow oil; yield, 46%; R_f = 0.29 (9 : 1 dichloromethane to methanol); ^1H NMR (400 MHz, CDCl_3) δ 8.71 (s, 1H), 7.85 (d, J = 7.1 Hz, 1H), 7.60 (d, J = 8.1 Hz, 1H), 7.53 (d, J = 5.3 Hz, 1H), 7.08 (d, J = 5.3 Hz, 1H), 5.69 (s, 1H), 4.84 (d, J = 5.7 Hz, 2H), 4.77 (d, J = 7.6 Hz, 1H), 4.05 (m, 1H), 1.14 (d, J = 6.5 Hz, 6H). ^{13}C NMR (101 MHz, CDCl_3) δ 161.85, 160.44, 157.36, 149.41, 147.19, 138.42, 136.49, 131.14, 123.86, 123.03, 120.39, 106.02, 43.16, 41.96, 23.13. HRMS: m/z calcd for $\text{C}_{16}\text{H}_{16}\text{F}_3\text{N}_5\text{NaS}$ [M + Na]⁺ 390.0971; found 390.0973.

C1 *N⁴-(4-Cyanobenzyl)-N²-isopropylpyrido[3,2-d]pyrimidine-2,4-diamine.* Yellow oil; yield, 62%; R_f = 0.56 (9 : 1 dichloromethane to methanol); ^1H NMR (400 MHz, CDCl_3) δ 8.28 (d, J = 3.4 Hz, 1H), 7.68 (d, J = 7.5 Hz, 1H), 7.57 (d, J = 7.9 Hz, 2H), 7.43 (d, J = 7.0 Hz, 2H), 7.40–7.30 (m, 1H), 5.19 (s, 1H), 4.80 (d, J = 5.9 Hz, 2H), 4.17 (m, 1H), 1.18 (d, J = 5.8 Hz, 6H). ^{13}C NMR (100 MHz, CDCl_3) δ 159.91, 158.77, 146.89, 144.35, 142.89, 132.24, 128.75, 127.98, 127.71, 118.75, 110.90, 72.69, 43.85, 42.83,



23.01. HRMS: m/z calcd for $C_{18}H_{19}N_6$ [M + H]⁺ 319.1666; found 319.1669.

C2 *N²-Isopropyl-N⁴-(2-(methylsulfonyl)benzyl)pyrido[3,2-d]pyrimidine-2,4-diamine.* White solid; yield, 71%; R_f = 0.49 (9 : 1 dichloromethane to methanol); ¹H NMR (400 MHz, CDCl₃) δ 8.30 (d, J = 4.2 Hz, 1H), 8.05 (d, J = 7.9 Hz, 1H), 7.75 (s, NH), 7.72 (d, J = 7.7 Hz, 1H), 7.65 (d, J = 8.4 Hz, 1H), 7.59 (t, J = 7.5 Hz, 1H), 7.48 (t, J = 7.6 Hz, 1H), 7.41 (dd, J = 8.5, 4.2 Hz, 1H), 5.17 (d, J = 6.5 Hz, 2H), 4.91 (s, NH), 4.28–4.18 (m, 1H), 3.17 (s, 3H), 1.24 (d, J = 6.5 Hz, 6H). ¹³C NMR (100 MHz, CDCl₃) δ 160.03, 158.90, 146.86, 143.35, 138.75, 138.43, 134.14, 132.35, 131.63, 130.08, 128.57, 127.86, 72.93, 45.27, 43.08, 42.06, 23.32. HRMS: m/z calcd for $C_{18}H_{22}N_5O_2S$ [M + H]⁺ 372.1489; found 372.1495. Melting point 161–162 °C.

C3 *N²-Isopropyl-N⁴-(4-(methylsulfonyl)benzyl)pyrido[3,2-d]pyrimidine-2,4-diamine.* Yellow oil; yield, 62%; R_f = 0.50 (9 : 1 dichloromethane to methanol); ¹H NMR (400 MHz, CDCl₃) δ 8.32–8.28 (m, 1H), 7.90 (d, J = 8.3 Hz, 2H), 7.70 (d, J = 8.4 Hz, 1H), 7.58 (d, J = 8.1 Hz, 2H), 7.44 (dd, J = 8.5, 4.2 Hz, 1H), 4.87 (d, J = 6.2 Hz, 2H), 4.18 (dt, J = 13.4, 6.7 Hz, 1H), 3.03 (s, 3H), 1.21 (d, J = 6.5 Hz, 6H). ¹³C NMR (100 MHz, CDCl₃) δ 160.00, 158.51, 145.20, 143.20, 139.61, 132.14, 128.36, 127.92, 127.78, 127.71, 72.80, 44.57, 43.91, 43.02, 23.06. HRMS: m/z calcd for $C_{18}H_{22}N_5O_2S$ [M + H]⁺ 372.1489; found 372.1491.

C5 *N²-Isopropyl-N⁴-(4-(trifluoromethyl)benzyl)pyrido[3,2-d]pyrimidine-2,4-diamine.* Yellow solid; yield, 91%; R_f = 0.55 (9 : 1 dichloromethane to methanol); ¹H NMR (400 MHz, CDCl₃) δ 8.31 (d, J = 4.2 Hz, 1H), 7.72 (d, J = 8.5 Hz, 1H), 7.60 (d, J = 8.1 Hz, 2H), 7.50 (d, J = 8.0 Hz, 2H), 7.45 (dd, J = 8.5, 4.2 Hz, 1H), 4.85 (d, J = 6.1 Hz, 2H), 4.21 (dq, J = 13.4, 6.7 Hz, 1H), 1.23 (d, J = 6.5 Hz, 6H). ¹³C NMR (101 MHz, CDCl₃) δ 160.00, 158.03, 143.44, 142.43, 130.35, 128.06, 127.98, 127.88, 125.57, 122.78, 72.81, 44.08, 43.19, 22.99. HRMS: m/z calcd for $C_{18}H_{19}F_3N_5$ [M + H]⁺ 362.1587; found 362.1595. Melting point 92–94 °C.

C13 *N²-Isopropyl-N⁴-((6-(trifluoromethyl)pyridin-3-yl)methyl)pyrido[3,2-d]pyrimidine-2,4-diamine.* Yellow solid; yield, 45%; R_f = 0.54 (9 : 1 dichloromethane to methanol); ¹H NMR (400 MHz, CDCl₃) δ 8.77 (s, 1H), 8.28 (dd, J = 4.2, 1.1 Hz, 1H), 7.88 (d, J = 7.9 Hz, 1H), 7.68 (d, J = 8.4 Hz, 1H), 7.63 (d, J = 8.1 Hz, 1H), 7.43 (dd, J = 8.5, 4.2 Hz, 1H), 4.94 (s, 1H), 4.85 (d, J = 6.2 Hz, 2H), 4.17 (d, J = 6.3 Hz, 1H), 1.20 (d, J = 6.4 Hz, 6H). ¹³C NMR (101 MHz, CDCl₃) δ 160.09, 158.83, 149.61, 147.54, 147.20, 147.10, 143.21, 137.97, 136.52, 132.68, 127.99, 123.05, 120.47, 43.08, 41.71, 23.19. HRMS: m/z calcd for $C_{17}H_{18}F_3N_6$ [M + H]⁺ 363.1540; found 363.1546. Melting point 111–113 °C.

D1 *N⁴-(4-Cyanobenzyl)-N²-isopropylpyrido[2,3-d]pyrimidine-2,4-diamine.* Yellow oil; yield, 24%; R_f = 0.32 (9 : 1 dichloromethane to methanol); ¹H NMR (400 MHz, CD₃OD) δ 8.53 (dd, J = 4.5, 1.6 Hz, 1H), 8.27 (d, J = 7.7 Hz, 1H), 7.59 (d, J = 8.1 Hz, 2H), 7.47 (d, J = 8.2 Hz, 2H), 7.00 (dd, J = 8.0, 4.6 Hz, 1H), 4.77 (s, 2H), 4.11 (s, 1H), 3.28–3.26 (m, 1H), 1.12 (d, J = 23.6 Hz, 6H). ¹³C NMR (101 MHz, CD₃OD) δ 162.49, 162.34, 161.84, 155.60, 146.66, 133.54, 133.28, 129.18, 119.76, 117.46, 111.56, 107.13, 45.26, 43.64, 23.06. HRMS: m/z calcd for $C_{18}H_{18}N_6Na$ [M + Na]⁺ 341.1485; found 341.1489.

D2 *N²-Isopropyl-N⁴-(2-(methylsulfonyl)benzyl)pyrido[2,3-d]pyrimidine-2,4-diamine.* Yellow solid; yield, 6%; R_f = 0.40 (9 : 1

dichloromethane to methanol); ¹H NMR (400 MHz, CD₃OD) δ 8.64–8.60 (m, 1H), 8.34 (d, J = 7.5 Hz, 1H), 8.05 (d, J = 7.8 Hz, 1H), 7.63 (d, J = 5.5 Hz, 2H), 7.51 (dd, J = 10.9, 5.5 Hz, 1H), 7.10 (dd, J = 7.9, 4.6 Hz, 1H), 5.22 (s, 2H), 4.18 (s, 1H), 3.31 (s, 3H), 1.12 (s, 6H). ¹³C NMR (101 MHz, CD₃OD) δ 162.64, 155.76, 151.44, 139.95, 139.49, 135.12, 133.48, 130.85, 130.57, 130.28, 130.08, 128.96, 117.56, 44.66, 30.82, 30.31, 22.99. HRMS: m/z calcd for $C_{18}H_{21}NaN_5O_2S$ [M + Na]⁺ 394.1308; found 394.1313.

D3 *N²-Isopropyl-N⁴-(4-(methylsulfonyl)benzyl)pyrido[2,3-d]pyrimidine-2,4-diamine.* Yellow solid; yield, 20%; R_f = 0.36 (9 : 1 dichloromethane to methanol); ¹H NMR (400 MHz, CD₃OD) δ 8.56 (dd, J = 4.6, 1.6 Hz, 1H), 8.30 (d, J = 7.7 Hz, 1H), 7.84 (d, J = 8.3 Hz, 2H), 7.57 (d, J = 8.3 Hz, 2H), 7.02 (dd, J = 8.0, 4.6 Hz, 1H), 4.82 (s, 2H), 3.30–3.27 (m, 1H), 3.04 (s, 3H), 1.14 (d, J = 34.1 Hz, 6H). ¹³C NMR (101 MHz, CD₃OD) δ 162.53, 162.33, 161.90, 155.62, 147.41, 140.48, 133.56, 129.21, 128.51, 117.47, 107.15, 45.16, 44.44, 43.64, 23.07. HRMS: m/z calcd for $C_{18}H_{21}NaN_5O_2S$ [M + Na]⁺ 394.1308; found 394.1311. Melting point 162–164 °C.

D5 *N²-Isopropyl-N⁴-(4-(trifluoromethyl)benzyl)pyrido[2,3-d]pyrimidine-2,4-diamine.* Yellow solid; yield, 74%; R_f = 0.47 (9 : 1 dichloromethane to methanol); ¹H NMR (400 MHz, DMSO-d₆) δ 8.72–8.44 (m, 1H), 8.44 (d, J = 42.8 Hz, 1H), 7.62 (d, J = 8.1 Hz, 2H), 7.52 (d, J = 7.9 Hz, 2H), 7.05 (d, J = 35.0 Hz, 1H), 4.74 (d, J = 4.3 Hz, 2H), 4.14–3.88 (m, 1H), 1.01 (dd, J = 23.4, 16.7 Hz, 6H). ¹³C NMR (101 MHz, DMSO-d₆) δ 166.89, 160.53, 144.22, 143.15, 131.44, 127.87, 127.60, 127.29, 125.65, 125.10, 122.95, 64.96, 62.77, 22.37. HRMS: m/z calcd for $C_{18}H_{18}F_3N_5Na$ [M + Na]⁺ 384.1407; found 384.1410. Melting point 107–110 °C.

D13 *N²-Isopropyl-N⁴-((6-(trifluoromethyl)pyridin-3-yl)methyl)pyrido[2,3-d]pyrimidine-2,4-diamine.* Yellow solid; yield, 7%; R_f = 0.26 (9 : 1 dichloromethane to methanol); ¹H NMR (400 MHz, CD₃OD) δ 8.76 (s, 1H), 8.64 (s, 1H), 8.39 (s, 1H), 8.06 (d, J = 8.0 Hz, 1H), 7.78 (d, J = 8.1 Hz, 1H), 7.17 (s, 1H), 4.90 (d, J = 2.4 Hz, 2H), 4.18 (d, J = 8.2 Hz, 1H), 1.15 (s, 6H). ¹³C NMR (101 MHz, CD₃OD) δ 162.36, 155.77, 150.41, 147.57, 140.24, 138.24, 133.92, 130.83, 127.14, 124.43, 121.67, 121.64, 119.00, 107.13, 64.33, 43.99, 43.20, 22.95. HRMS: m/z calcd for $C_{17}H_{17}F_3N_6Na$ [M + Na]⁺ 385.1359; found 385.1366. Melting point 108–110 °C.

Antibacterial activities assay

Bacterial strains and growth conditions. *E. coli* CMCC 44102, *S. aureus* ATCC 6538, *S. epidermidis* ATCC 12228, *S. typhimurium* CMCC 50115 and MRSA ATCC 43300 used in this study were acquired from Guangdong Microbiology Culture Center. *E. coli*, *S. aureus*, *S. epidermidis* and MRSA were grown in Mueller-Hinton Broth (MHB) and *S. typhimurium* was grown in tryptic soy broth (TSB) at 37 °C, and agar was added to a final concentration of 1.5% (w/v) for growth plates.²⁵

Kirby-Bauer assay. These assays for antibacterial activity were performed as reported previously.^{25,33} Briefly, streaked bacterial strains were put onto agar plates and incubated overnight. A single colony was picked to inoculate into broth media and incubated overnight. The activated broth cultures were diluted 1 : 1000 into 5 mL of broth media. 400 μL of diluted culture was added to an agar plate with a diameter of 120 mm



and was coated uniformly, allowed to dry for 15 min before use. After that, nine sterile filter disks with a diameter of 6 mm were added and 5 μ L of 5 mg mL⁻¹ test compound dissolved in DMSO were dropwise added to each filter disk. Bacterial plates were incubated overnight. The assays were performed in triplicate and zones of inhibition were measured in millimeters.

Microtiter MIC determination assay. Two assays were carried out based on previous methods.^{25,33} The minimum inhibitory concentrations (MIC) were determined for compounds which showed antibacterial activity against corresponding strains. Broth cultures were prepared as above and 1000 fold diluted cultures were added to a sterile 96-well plate with a dosage of 200 μ L per well. 5 μ L compounds, with two-times gradient dilution, were added to wells and mixed by pipetting, then, the plates were incubated at 37 °C overnight. MICs were determined by visual inspection of minimum concentration of compound inhibiting bacterial growth. Each concentration was performed parallelly in triplicate to verify the MIC determinations. Pure DMSO was used as blank control which didn't show inhibition about bacterial growth.

DMPK properties assays

The DMPK properties data described above were measured through a high through-put platform kindly provided by AstraZeneca U.K. The methods of the five assays, including log $D_{7.4}$, aqueous solubility, plasma protein binding, microsome and hepatocyte clearance measurements has been reported previously (Basarab *et al.*, 2014 and Doyle *et al.*, 2016) and are described briefly as below^{34,35}.

log $D_{7.4}$ Determination assay. The partition coefficient (log D) was measured by shake flask method, using 10 mM phosphate buffer at pH 7.4 and *n*-octanol. The samples were allowed to reach equilibrium by shaking for 1 hour at 1200 rpm, and sample analysis was done by LC/UV, with MS for mass confirmation.

Aqueous (thermodynamic) solubility assay. It is a shake-flask approach that uses compounds dried from 10 mM DMSO solutions. The dried compounds are equilibrated in an aqueous phosphate buffer (pH 7.4) for 24 hours at 25 °C, the portion with the dissolved compound is then separated from the remains. The solutions are analysed and quantified using UPLC/MS/MS.

Plasma protein binding determination assay. Human plasma protein binding was determined from a 10 μ M compound solution in a Dianorm plasma well incubating at 37 °C for 16 hours. Free fractions were calculated from ratios of drug concentration in buffer and plasma wells determined by LC-MS/MS.

In vitro hepatocyte and microsomal clearance assays. Cryopreserved or fresh hepatocytes were incubated with test compounds at a final concentration of 1 μ M in incubation medium containing 1.0×10^6 viable cells per mL (hepatocyte incubations) or with a microsomal protein concentration of 1 mg mL⁻¹ + 1 mM NADPH. Incubations were performed at 37 °C and samples taken at 5, 15, 30, 45, 60, 80, 100 and 120 min (hepatocytes) and 0.5, 5, 10, 15, 20 and 30 min (microsomes) for analysis using LC-MS/MS. Peak areas were determined from

extracted ion chromatograms and the *in vitro* half-life ($t_{1/2}$) of parent compound determined by regression analysis of the ln percent parent disappearance vs. time curve. The *in vitro* intrinsic clearance (*in vitro* CL_{int}, in μ L min⁻¹ per 10^6 cells or mg protein) was determined from the slope value using the following equation: *in vitro* CL_{int} = kV/N where V = incubation volume; N = number of hepatocytes or protein concentration per well.

Conflicts of interest

Compounds described in this manuscript are included in a UK patent application filed by the Liverpool School of Tropical Medicine and the University of Liverpool (application No. 1700814.5, filed 17 January 2017). The authors declare that they have no other competing interests.

Acknowledgements

The authors want to thank the DMPK group (led by Peter Webborn) in AstraZeneca U.K. for providing the *in vitro* measurement of DMPK properties, including log $D_{7.4}$, aqueous solubility, human plasma protein binding, mouse microsome clearance and rat hepatocytes clearance of hit and lead molecules. Majority of the synthetic and biological research work was carried out in the Liverpool-GDUT Joint Laboratory for Drug Discovery located in Guangdong University of Technology (GDUT). Financial support was provided by the Guangzhou Municipal Science and technology project for major project of industry-university-research cooperation and collaborative innovation (project No. 2016201604030025), Liverpool-GDUT Drug Discovery Initiative (project No. CA131122SWGDUT), the Department of Science and Technology of Guangdong province (project No. 2017A050501034), the Department of Education of Guangdong Province (project No. 2013JDXM27) and Guangzhou Science and Technology Plan (project No. 201604030020 and No. 2017A050501034). Compounds described in this manuscript are included in an UK Patent Application No. 1700814.5.

References

- 1 C. Walsh, *Nat. Rev. Microbiol.*, 2003, **1**, 65–70.
- 2 L. Feng, M. M. Maddox, M. Z. Alam, L. S. Tsutsumi, G. Narula, D. F. Bruhn, X. Wu, S. Sandhaus, R. B. Lee, C. J. Simmons, Y. C. Tse-Dinh, J. G. Hurdle, R. E. Lee and D. Sun, *J. Med. Chem.*, 2014, **57**, 8398–8420.
- 3 L. G. M. Bode, J. A. J. W. Kluytmans, H. F. L. Wertheim, D. Bogaers, C. M. J. E. Vandebroucke-Grauls, R. Roosendaal, A. Troelstra, A. T. A. Box, A. Voss, I. van der Tweel, A. van Belkum, H. A. Verbrugh and M. C. Vos, *N. Engl. J. Med.*, 2010, **362**, 9–17.
- 4 H. Mohammad, P. V. Reddy, D. Monteleone, A. S. Mayhoub, M. Cushman and M. N. Seleem, *Eur. J. Med. Chem.*, 2015, **94**, 306–316.
- 5 S. M. Lehar, T. Pillow, M. Xu, L. Staben, K. K. Kajihara, R. Vandlen, L. DePalatis, H. Raab, W. L. Hazenbos, J. H. Morisaki, J. Kim, S. Park, M. Darwish, B. C. Lee,



H. Hernandez, K. M. Loyet, P. Lupardus, R. Fong, D. Yan, C. Chalouni, E. Luis, Y. Khalfin, E. Plise, J. Cheong, J. P. Lyssikatos, M. Strandh, K. Koefoed, P. S. Andersen, J. A. Flygare, M. Wah Tan, E. J. Brown and S. Mariathasan, *Nature*, 2015, **527**, 323–328.

6 S. R. Martinez, D. M. Rocca, V. Aiassa and M. C. Becerra, *RSC Adv.*, 2016, **6**, 101023–101028.

7 H. F. Chambers and F. R. Deleo, *Nat. Rev. Microbiol.*, 2009, **7**, 629–641.

8 B. A. Diep, S. R. Gill, R. F. Chang, T. H. Phan, J. H. Chen, M. G. Davidson, F. Lin, J. Lin, H. A. Carleton, E. F. Mongodin, G. F. Sensabaugh and F. Perdreau-Remington, *Lancet*, 2006, **367**, 731–739.

9 L. C. Chan, A. Gilbert, L. Basuino, T. M. da Costa, S. M. Hamilton, K. R. Dos Santos, H. F. Chambers and S. S. Chatterjee, *Antimicrob. Agents Chemother.*, 2016, **60**, 3934–3941.

10 R. J. Guidos, B. Spellberg, M. Blaser, H. W. Boucher, J. S. Bradley, B. I. Eisenstein, D. Gerding, R. Lynfield, L. B. Reller, J. Rex, D. Schwartz, E. Septimus, F. C. Tenover, D. N. Gilbert and IDSA, *Clin. Infect. Dis.*, 2011, **52**, S397–S428.

11 J. P. Surivet, C. Zumbrunn, G. Rueedi, D. Bur, T. Bruyere, H. Locher, D. Ritz, P. Seiler, C. Kohl, E. A. Ertel, P. Hess, J. C. Gauvin, A. Mirre, V. Kaegi, M. Dos Santos, S. Kraemer, M. Gaertner, J. Delers, M. Enderlin-Paput, M. Weiss, R. Sube, H. Hadana, W. Keck and C. Hubschwerlen, *J. Med. Chem.*, 2015, **58**, 927–942.

12 R. J. Gordon and F. D. Lowy, *Clin. Infect. Dis.*, 2008, **46**(suppl. 5), S350–S359.

13 C. Vuong, A. J. Yeh, G. Y. Cheung and M. Otto, *Expert Opin. Invest. Drugs*, 2016, **25**, 73–93.

14 C. M. Macal, M. J. North, N. Collier, V. M. Dukic, D. T. Wegener, M. Z. David, R. S. Daum, P. Schumm, J. A. Evans, J. R. Wilder, L. G. Miller, S. J. Eells and D. S. Lauderdale, *J. Transl. Med.*, 2014, **12**, 124–135.

15 L. M. Weigel, D. B. Clewell, S. R. Gill, N. C. Clark, L. K. McDougal, S. E. Flannagan, J. F. Kolonay, J. Shetty, G. E. Killgore and F. C. Tenover, *Science*, 2003, **302**, 1569–1571.

16 M. K. Hayden, K. Rezai, R. A. Hayes, K. Lolans, J. P. Quinn and R. A. Weinstein, *J. Clin. Microbiol.*, 2005, **43**, 5285–5287.

17 G. Morales, J. J. Picazo, E. Baos, F. J. Candel, A. Arribi, B. Pelaez, R. Andrade, M. A. de la Torre, J. Fereres and M. Sanchez-Garcia, *Clin. Infect. Dis.*, 2010, **50**, 821–825.

18 L. C. Chan, L. Basuino, B. Diep, S. Hamilton, S. S. Chatterjee and H. F. Chambers, *Antimicrob. Agents Chemother.*, 2015, **59**, 2960–2963.

19 W. H. Organization, *WHO publishes list of bacteria for which new antibiotics are urgently needed*, <http://www.who.int/mediacentre/news/releases/2017/bacteria-antibiotics-needed/en/>.

20 D. Wang and F. Gao, *Chem. Cent. J.*, 2013, **7**, 95–109.

21 E. Jafari, M. R. Khajouei, F. Hassanzadeh, G. H. Hakimelahi and G. A. Khodarahmi, *Res. Pharm. Sci.*, 2016, **11**, 1–14.

22 Y. L. Gao, Q. Z. Xiong, R. An and X. P. Bao, *Chin. J. Org. Chem.*, 2011, **31**, 1529–1537.

23 P. M. Bedi, V. Kumar and M. P. Mahajan, *Bioorg. Med. Chem. Lett.*, 2004, **14**, 5211–5213.

24 P. M. Chandrika, T. Yakaiah, G. Gayatri, K. P. Kumar, B. Narsaiah, U. S. N. Murthy and A. R. R. Rao, *Eur. J. Med. Chem.*, 2010, **45**, 78–84.

25 K. S. Van Horn, W. N. Burda, R. Fleeman, L. N. Shaw and R. Manetsch, *J. Med. Chem.*, 2014, **57**, 3075–3093.

26 D. Gonzalez Cabrera, C. Le Manach, F. Douelle, Y. Younis, T. S. Feng, T. Paquet, A. T. Nchinda, L. J. Street, D. Taylor, C. de Kock, L. Wiesner, S. Duffy, K. L. White, K. M. Zabiulla, Y. Sambandan, S. Bashyam, D. Waterson, M. J. Witty, S. A. Charman, V. M. Avery, S. Wittlin and K. Chibale, *J. Med. Chem.*, 2014, **57**, 1014–1022.

27 M. T. Kenji Yoshida, *J. Chem. Soc. Pak.*, 1992, **1**, 919–923.

28 K. Kanuma, K. Omodera, M. Nishiguchi, T. Funakoshi, S. Chaki, Y. Nagase, I. Iida, J. Yamaguchi, G. Semple, T. A. Tran and Y. Sekiguchi, *Bioorg. Med. Chem.*, 2006, **14**, 3307–3319.

29 P. R. Gilson, C. Tan, K. E. Jarman, K. N. Lowes, J. M. Curtis, W. Nguyen, A. E. Di Rago, H. E. Bullen, B. Prinz, S. Duffy, J. B. Baell, C. A. Hutton, H. Jousset Subroux, B. S. Crabb, V. M. Avery, A. F. Cowman and B. E. Sibley, *J. Med. Chem.*, 2017, **60**, 1171–1188.

30 X. Zhu, K. S. Van Horn, M. M. Barber, S. Yang, M. Z. Wang, R. Manetsch and K. A. Werbovetz, *Bioorg. Med. Chem.*, 2015, **23**, 5182–5189.

31 W. Devine, J. L. Woodring, U. Swaminathan, E. Amata, G. Patel, J. Erath, N. E. Roncal, P. J. Lee, S. E. Leed, A. Rodriguez, K. Mensa-Wilmot, R. J. Sciotti and M. P. Pollastri, *J. Med. Chem.*, 2015, **58**, 5522–5537.

32 K. L. Johnston, D. A. N. Cook, N. G. Berry, W. David Hong, R. H. Clare, M. Goddard, L. Ford, G. L. Nixon, P. M. O'Neill, S. A. Ward and M. J. Taylor, *Sci. Adv.*, 2017, **3**, 1551–1560.

33 W. N. Burda, K. B. Fields, J. B. Gill, R. Burt, M. Shepherd, X. P. Zhang and L. N. Shaw, *Eur. J. Clin. Microbiol. Infect. Dis.*, 2012, **31**, 327–335.

34 G. S. Basarab, P. J. Hill, C. E. Garner, K. Hull, O. Green, B. A. Sherer, P. B. Dangel, J. I. Manchester, S. Bist, S. Hauck, F. Zhou, M. Uria-Nickelsen, R. Illingworth, R. Alm, M. Rooney and A. E. Eakin, *J. Med. Chem.*, 2014, **57**, 6060–6082.

35 K. Doyle, H. Lonn, H. Kack, A. Van de Poel, S. Swallow, P. Gardiner, S. Connolly, J. Root, C. Wikell, G. Dahl, K. Stenvall and P. Johannesson, *J. Med. Chem.*, 2016, **59**, 9457–9472.

